Proceedings of the Federated Conference on
Computer Science and Information Systems pp. 117–122

ISBN 978-83-60810-51-4

# Estimation of Eye Condition using Waveform Shapes of Pupil Light Responses to Chromatic Stimuli

Minoru Nakayama*, Wioletta Nowak†, Hitoshi Ishikawa‡, Ken Asakawa‡ and Yoshiaki Ichibe§
* Human System Science, The Graduate School of Decision Science & Technology
Tokyo Institute of Technology, Meguro, Tokyo 152-8552 Japan
Email: nakayama@cradle.titech.ac.jp
† Biomedical Engineering and Instrumentation, Wroclaw University of Technology, Wroclaw 50-370, Poland
Email: Wioletta.Nowak@pwr.wroc.pl
‡ Department of Orthoptics and Visual Science, Kitasato University, Sagamihara, Kanagawa 228-8555, Japan
§ School of Medicine, Kitasato University, Sagamihara, Kanagawa 228-8555, Japan

***Abstract*—This paper examines the possibility of detecting 2 conditions which cause vision to deteriorate: Aged-Related Macular Degeneration (AMD), and the effects of aging on eyes using the features of PLR waveforms. These features were extracted using Fourier descriptors of PLR waveform shapes, weighted amplitudes of the waveforms, and a balanced combination of these two in the from of a weighted value. The Random Forest method was used for classification analysis to detect three types of PLR, such as in healthy eyes, in AMD-affected eyes, and in age-affected eyes. The optimized weight values were evaluated using a classification error rate. The results show that the error rates for healthy PLRs and AMD PLRs were low, but the error rates for PLRs of age-affected eyes stayed at a high level. Additionally, dissimilarities between the PLRs for blue light and red light at low intensities contributed to the performance of the classification technique.**

***Index Terms*—Pupil Light Reflex; Age-Related Macular Degeneration; Waveform shape; Fourier Descriptors; Random Forests**

## I. Introduction

THE pupil light reflex (PLR) to chromatic stimuli has been analyzed since the discovery of the melanopsin-associated photoreceptive system (intrinsically photosensitive retinal ganglion cell pRGCs) in the human retina [2]. In particular, the difference between the response behavior of this photoreceptive system and that of the conventional rod-cone system has been compared [1], [3]. The differences in the PLR waveforms caused by the sensitivity and activity of these cells provides the possibility of proposing a diagnostic procedure for clinical examination of the retina [4], [15]. It is supposed that retinal diseases such as Age-related Macular Degeneration (AMD) [13] and the effects of aging on eyes, or age-affected eyes influence PLR waveforms, and that an evaluation procedure may be developed to detect the resulting irregular responses [10].

The procedure employs Multi Dimensional Scaling (MDS) techniques [12], [14] to classify individual differences in PLRs [9]. The features of PLR waveform shapes are extracted using the Fourier descriptor technique [11], [16], [17]. Additionally, a detection procedure for AMD patients using feature differences between left and right pupil responses has been proposed, as in most cases only one eye has the disease. However, this procedure can not be used in cases where both eyes are diseased.

In this paper, feature expressions of PLRs are modified to identify pupil characteristics, by considering the degree of amplitude of the PLR. Also, a classification technique has been introduced to detect AMD affected eyes using the Random Forest method [5].

## II. Method

### A. Subjects

In this experiment, 7 healthy young subjects (20–21 years old) and 6 elderly AMD-affected patients (59–86 years old) participated. Each elderly patient had a diseased eye and a healthy eye. Diseased eyes with choroidal neovascularization (CNV) in the macular region are often affected by new blood vessels, which bleed and form dense macular scars [13]. Also, CNV is a major cause of visual loss due to AMD [13].

All subjects participated in this experiment voluntarily, and agreed to the experimental procedure before it commenced.

### B. Experimental procedure

Pupil responses were measured using the PLR observation procedure, to determine the level of functionality of the melanopsin-associated photo-receptors [4], [15]. In the experiment, a long wavelength (635nm bandwidth) red light and a short wavelength (470nm bandwidth) blue light were used at 2 different light intensities (10 $cd/m^2$ and 100 $cd/m^2$). Pupil responses were recorded using Hamamatsu Iriscorder Dual equipment at a sampling rate of 30 Hz. The observation period consisted of a 10 second light pulse which caused a restriction of the pupil size, followed by 10 seconds without a light pulse during which restoration of the pupil size was allowed to occur. The light pulses were projected within the

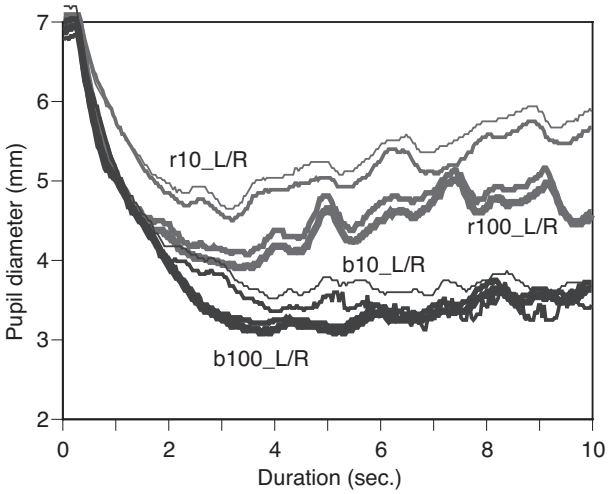


Fig. 1. PLR of both eyes of a healthy subject.

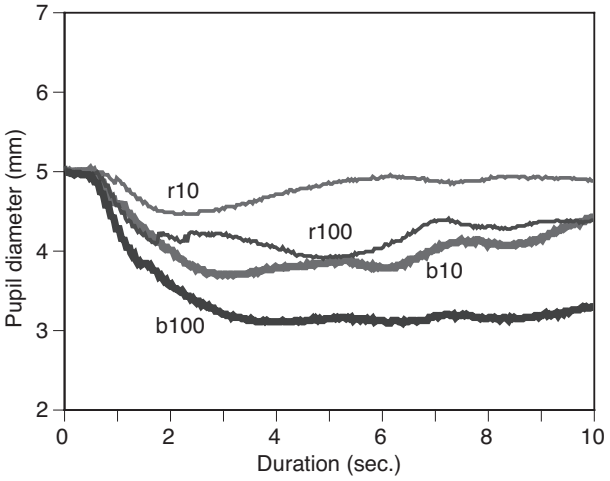


Fig. 2. PLR of a diseased eye.

housing of a pair of goggles. The measurements were taken in a darkened room, after a 5 minute darkness adaptation period. Responses for both left and right pupils were recorded for each subject. In this paper, the four conditions for the left (L) and right (R) eyes are defined as follows: r10 (long wavelength & low light intensity), r100 (long & high intensity), b10 (short wavelength & low intensity), and b100 (short wavelength & high intensity). The pupil responses for a healthy subject are illustrated in Figure 1, and the pupil responses for a patient with AMD-affected are illustrated in Figure 2.

### C. Extraction of waveform features

The features for PLR waveforms can be noted using the Fourier Discrete Transform (DFT) [8], [9].

$$x(n) = a_0 + \sum_{k=1}^{N/2}(a(k)cos(2\pi k\frac{t(n)}{N\Delta}) + b(k)sin(2\pi k\frac{t(n)}{N\Delta})) \quad (1)$$

The PLR waveforms can be represented using coefficients $a_0$, a(k) and b(k) with periodical sine and cosine functions. The magnitude of a(k) and b(k) is noted as $FD$, and given as $FD_i(i = 0, \ldots, N/2-1)$. The feature vector of the waveform shape can be defined using $FD$. This method of presentation is known as a Fourier Descriptor [11], [16], [17].

In general, the component $FD_0$, $a_0$ in the equation shows the DC component of the signal, corresponding to the signal amplitude. The remaining components of $FD$ describe the shape of the waveform. The components are affected by individual factors, so that a standardized feature using $FD_1$ as a vector is preferred [17].

It is suggested that low-order values of 4 or 5 FDs can represent the characteristics of waveform shapes [11], thus 4 components are extracted as feature vectors ($f$). For example, feature vectors for the left eye of the healthy subject in Figure 1 can be noted as follows:

$$f_{r10\_L} = [0.61, 0.34, 0.28, 0.36]$$
$$f_{r100\_L} = [0.68, 0.52, 0.40, 0.36]$$
$$f_{b10\_L} = [0.68, 0.47, 0.48, 0.33]$$
$$f_{b100\_L} = [0.64, 0.43, 0.33, 0.30]$$

### D. Feature modification

In a comparison of the two sets of waveforms in Figures 1 and 2, the amplitudes of the waveforms are different between healthy and AMD affected subjects. The features are generated from waveform shapes which exclude the DC component, though the amplitude of the waveform has not been sufficiently considered as a feature. To include $FD_0$ components with features, the $FD_0$ values were standardized using the mean for each eye. In case of the left eye of the healthy subject in Figure 1, the $FD_0{}'$ of the standardized $FD_0$ is noted as follows:

$$[FD_{0:r10\_L}{}'FD_{0:r100\_L}{}'FD_{0:b10\_L}{}'FD_{0:b100\_L}{}'] = [0.65, 0.95, 1.16, 1.25]$$

Combined vector $f'$ can be noted using coefficient $w$.

$$f' = [\frac{FD_2}{FD_1}, \frac{FD_3}{FD_1}, \ldots, \frac{FD_5}{FD_1}, wFD_0{}']$$

Here, $w$ is a coefficient used as a weighted value to create a balance between features of waveform shapes and standardized $FD_0$ ($FD_0{}'$). The performance of the classification is evaluated in response to $w$.

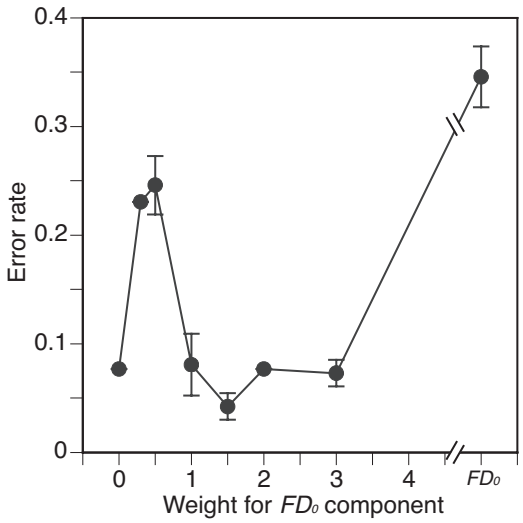


Fig. 3. Two-class classification error rate across $w$ values.

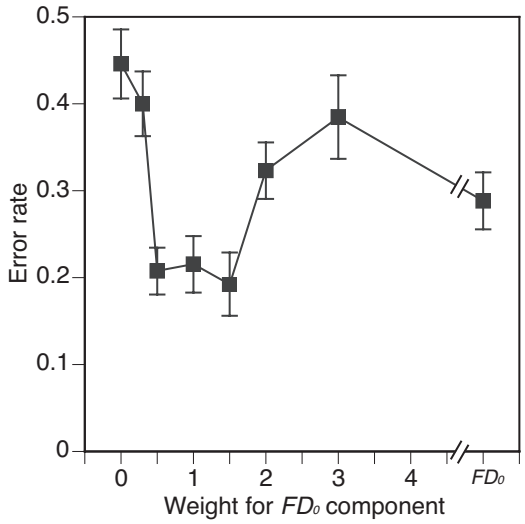


Fig. 4. Three-class classification error rate across $w$ values.

TABLE I
CONTINGENCY TABLE FOR TWO-CLASSES

| | D | H | Err. |
|---|---|---|---|
| AMD (D:N=6) | 5 | 1 | 0.17 |
| Healthy (H:N=20) | 0.1 | 19.9 | 0.005 |

$(FD_0{}'w = 1.5)$

TABLE II
CONTINGENCY TABLE FOR THREE-CLASSES

| | D | A | H | Err. |
|---|---|---|---|---|
| AMD (D:N=6) | 5 | 0 | 1 | 0.17 |
| Aged (A:N=6) | 0.9 | 2.9 | 2.2 | 0.52 |
| Healthy (H:N=14) | 0 | 0.9 | 13.1 | 0.06 |

$(FD_0{}'w = 1.5)$

### *E. Classification procedure*

In this paper, the number of subjects is small, and the number of trials for taking measurements is limited because the experimental stimuli influences the response. The Random Forest method [5], which uses an ensemble learning procedure to analyze the classification of the small samples, is frequently used. Also, the Random Forest method can show contributions of features and can conduct cross validation calculations. Since the structure of the feature data set is not clear, the results from the Random Forest method may provide useful information to improve the detection procedure. The statistical package R and the "RandomForest" package [6], [7] was used for this analysis.

The number of decision trees was set at 500 as a default value, and the sample size was set at 6. The total number of samples was 26 $(2 \times (6+7))$. One third of the samples were assigned as test data, and the rest of data was assigned as OOB (Out of Bag) training data. The selection of the data set was initially random. This selection was performed 10 times in order to calculate the generalized performance of the data throughout all conditions. The performance was evaluated according to the value of $w$, as follows:

$$w = [0, 0.3, 0.5, 1.0, 1.5, 2.0, 3.0, \infty]$$

Here, $\infty$ means a case using only $FD_0{}'$.

Classification of the modified set of features into 2-classes: Healthy (H) and AMD (D), or into 3-classes: Healthy (H), AMD (D) and age-affected eyes (A) was conducted using the RF technique.

According to the preliminary analysis, the performance was low when the feature set of equation (1) was used. Next, Euclidean distances among the four conditions were analyzed in the same way as in the previous assessment [10].

Here, an Euclidean distance matrix is shown as $Ed_{Healthy\ L}$ for the example of the healthy subject, and the distance feature is noted as $FE$.

$$Ed_{Healthy\ L} = \begin{array}{c|cccc} & r10 & r100 & b10 & b100 \\ \hline r10 & 0 & 0.37 & 0.57 & 0.62 \\ r100 & 0.37 & 0 & 0.24 & 0.33 \\ b10 & 0.57 & 0.24 & 0 & 0.18 \\ b100 & 0.62 & 0.33 & 0.18 & 0 \end{array}$$

$$FE = [r10 - r100, r10 - b10, r10 - b100, r100 - b10, r100 - b100, b10 - b100]$$

$$FE_{Healthy\ L} = [0.37, 0.57, 0.62, 0.24, 0.33, 0.18]$$

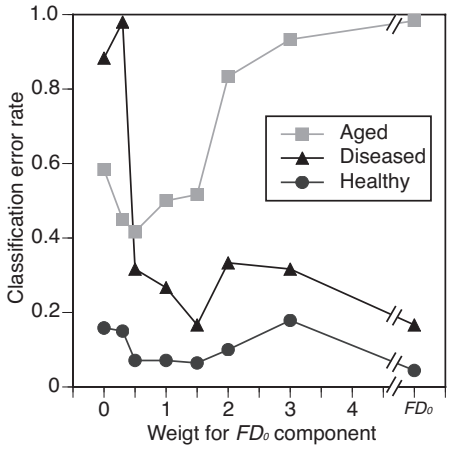


Fig. 5. Error rates for classification of each class.

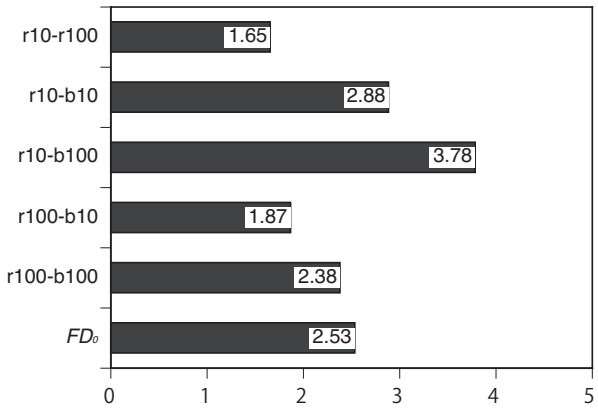


Fig. 6. Comparison of contribution values across features ($w$=1.5).

## III. Results

### A. 2-class performance

For two-class classification of PLRs of Healthy (H) and AMD-affected (D) eyes, 10 times calculations were conducted using $w$ values. Mean error rates of classification are summarized in Figure 3. The horizontal axis shows weight $w$, and the vertical axis shows the error rate. The error bar in the figure shows the standard deviation (STD). The minimum error rate appears at $w = 1.5$. In the case of $w = 0.5$ or only $FD_0{}'$, the error rates are high.

The estimation performance for $w = 1.5$ is summarized as a contingency table in Table I. The table shows that healthy eyes can almost always be correctly classified, but the error rate of classification for AMD-affected eyes is low, at 17%.

### B. 3-class performance

Three class classification of PLRs of Healthy (H), AMD-affected (D) and age-affected (A) eyes, 10 times calculations were conducted using $w$ values. Mean error rates across $w$ values are summarized in Figure 4 using the same format as in Figure 3. Error bars in the figure show the STD of all 10 results. The minimum error rate also appears when $w = 1.5$, while the rate changes with the $w$ values.

The results for 3 classes are summarized as a contingency table in Table II, as mean rates for all 10 results. According to the results, healthy eyes are almost always correctly classified, while the error rate for AMD-affected eyes is low again, at 17%. The performance for age-affected eyes is not good, as the error rate is over 50%. The age-affected eyes class may include eyes which respond in the same manner as eyes of young people or eyes whose condition is similar to AMD affected eyes. Therefore, further observation of the condition of the subject's eyes may be required.

The error rates for the three classes are summarized in Figure 5. The rates of both Healthy and AMD-affected eyes are almost always small, and the minimum rate appears at $w = 1.5$. The rates for age-affected eyes are relatively higher than the ones for the other two classes.

### C. Contributing features for estimations

According to the classification results in the previous section, pupils can be classified accurately using features of PLR waveforms, except for the performance of age-affected eyes.

The next question was which components of features make it possible to classify PLRs. After that, the contributions of features were evaluated using the Random Forest tool. The degrees of contribution for each feature are summarized in Figure 6. The figure suggests that Euclidean distances are dissimilar between PLRs for blue light and PLRs for red light at low intensities such as $r10 - b100$ or $r10 - b10$, and denote the level of performance. Also, color differences at high intensities in PLRs such as $r100 - b100$, or amplitudes of $FD_0{}'$ present the ability to distinguish the type of pupil.

These results coincide with the visual differences in PLRs between healthy and AMD-affected patients.

### D. Clustered PLRs

The similarities of the features of waveform shapes in PLRs are also identified using the Random Forest procedure, then cluster analysis of these distances is conducted using the Ward method. Figure 7 shows a resulting dendrogram of the clusters of PLR features with $w = 1.5$ as the optimized value. In this figure, all subjects and eyes are indicated as Healthy/Patient and Left/Right or Normal/Diseased.

As the figure shows, the upper cluster displays a group of healthy subjects except for one a patient with age-affected eyes. A sub-cluster consists of both eyes of most subjects. The lower clusters consist of patients with age-affected eyes in the upper part and patients with AMD-affected eyes in the lower part. Some healthy subjects and some patients with AMD-affected eyes have been incorrectly classified into these groups. These occurrences have been explained in the above section where performance was classified.

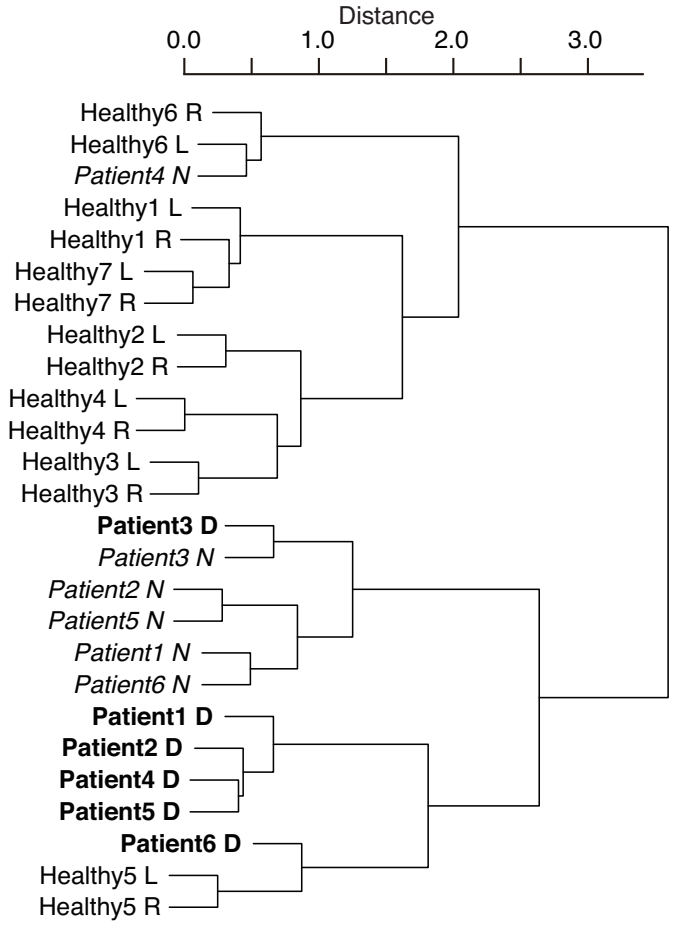


Fig. 7. Results of clustering of PLRs of all subjects ($w$=1.5).

To improve the performance of the test, responses should be opthalmologically diagnosed. For the classification procedures, many different data mining tools have been developed, so a more effective procedure should be devised. The characteristics of features of pupillary response waveform shapes which result from using the Random Forest method. They will be a subject of our further study.

## IV. Conclusion

This paper determined the possibility of detecting AMD-affected eyes and age-affected eyes using features of PLR waveforms. These features consist of Fourier descriptors of PLR waveform shapes and their amplitudes, and a balanced combination of these two was controlled using weighted values. The Random Forest method of classification analysis of the PLR waveform feature dissimilarities was conducted across the four types of stimuli. The weighted values were optimized using variations of the classification error rate.

In the results, the error rates for healthy pupils and AMD-affected pupils were low when the value of the coefficient was optimized as 1.5. However, the error rates for patients with age-affected eyes was high. The contributions of the components of these features were evaluated, and the differences between PLRs for blue light and PLRs for red light at low intensities strongly contributed to the classification.

Pupils of patients with age-affected eyes were influenced by various factors, so it may not be easy to classify healthy and AMD-affected patients in these cases. Additional feature processing may be required. This will be a subject of our further study in the near future.

## References

[1] D. M. Dacey, H. W. Liao, B. B. Peterson, "Melanopsin-expressing ganglion cells in primate retina signal color and irradiance and project to the LGN", *Nature*, 433, 749–754, 2005.

[2] P. D. Gamlin, D. H. McDougal, J. Pokorny, "Human and macaque pupil responses driven by melanopisn-containing retinal ganglion cells", *Vision Research*, 47, 946–954, 2007.

[3] S. Hattar, H. W. Liao, M. Takao, "Melanopsin-containing retinal ganglion cells: architecture, projections, and intrinsic photosensitivity", *Science*, 295, 1065–1070, 2002.

[4] A. Kawasaki, R. H. Kardon, "Intrinsically photosensitive retinal ganglion cells", *Journal of Neuro-Opthalmology*, 27, 195–204, 2007.

[5] J. Mingzhe, M. Murakami, "Authorship Identification Using Random Forests", *Proceedings of the Institute of Statistical Mathematics*, 55(2), 255–268, 2007.

[6] J. Mingzhe, "Toukeiteki Tekisuto Kaiseki 15", *ESTRELA*, No.182, 44–49, 2009.

[7] Package "randomForest", http://stat-www.berkeley.edu/users/breiman/RandomForests
[8] I. Morishita, H. Kobatake, *Signal Processing*, The Society of Instrument and Control Engineers, Tokyo, Japan, 1982.
[9] M. Nakayama, W. Nowak, H. Ishikawa, K. Asakawa, "An Assessment Procedure Involving Waveform Shapes for Pupil Light Reflex", *Proceedings of BIOSIGNALS2010*, 322-326, 2010.
[10] M. Nakayama, W. Nowak, H. Ishikawa, K. Asakawa, Y. Ichibe, "Waveform Shapes for Pupil Light Responses and Their Analyzing Procedure", IEICE Technical Report, MBE2010-103, 1–6, 2011.
[11] B. Pinkowski, "Robust fourier descriptions for characterizing amplitude-modulated waveform shapes", *Journal of Acoustical Society of America*, 95(6), 3419–3423, 1994.
[12] J. Leeuw, P. Mair, "Multidimensional Scaling Using Majorization: SMACOF in R", *Journal of Statistical Software*, 31(3), 2009.
[13] J.Z. Nowak, "Age-related macular degeneration (AMD): pathogenesis and therapy", *Phamacological Reports*, 58, 353-363, 2006.
[14] Y. Takane, "Applications of multidimensional scaling in psychometrics", In Rao, C. and Sinharay, S., editors, *handbook of statistics 26 – Psychometrics*, 359–400. North-Holland, Amsterdam, Netherlands, 2007.
[15] R. Young, E. Kimura, "Pupillary correlates of light-evoked melanopsin activity in humans", *Vision Research*, 48, 862–871, 2008.
[16] C. T. Zahn, R. Z. Roskies, "Fourier descriptors for plane closed curves", *IEEE Transaction on Computers*, C-21(3), 269–281, 1971.
[17] D. Zhang, G. Lu, "A comparative study on shape retrieval using fourier descriptors with different shape signatures", *Proceedings of the 5th Asian Conference on Computer Vision*, 646–651. Springer, 2002.